Korean J. Chem. Eng., 32(2), 248-254 (2015)
DOI: 10.1007/s11814-014-0215-z

pISSN: 0256-1115
eISSN: 1975-7220

Preparation of activated carbon aerogel and its application to electrode material for electric double layer capacitor in organic electrolyte: Effect of activation temperature

Soon Hyung Kwon*, Eunji Lee*, Bum-Soo Kim, Sang-Gil Kim**, Byung-Jun Lee**, Myung-Soo Kim*,†, and Ji Chul Jung*,†**

*Department of Chemical Engineering, Myongji University, Yongin 449-728, Korea
**R&D Center, Vitzrocell Co., Ltd., Chungnam 340-861, Korea
(*Received 16 June 2014 • accepted 26 July 2014*)

Abstract−Carbon aerogel was chemically activated with KOH at various activation temperatures with the aim of improving the electrochemical performance of carbon aerogel for EDLC electrode. Electrochemical performance of activated carbon aerogel electrode was determined by cyclic voltammetry and galvanostatic charge/discharge methods using coin-type EDLC cell in organic electrolyte. Activation temperature played an important role in determining the electrochemical performance of activated carbon aerogel for EDLC electrode. Specific capacitance of activated carbon aerogel at a high current density (5 A/g) showed a volcano-shaped curve with respect to activation temperature. Excessively high activation temperature could have an adverse effect on the electrochemical properties of activated carbon aerogel due to the low electrical conductivity caused by a collapse of characteristic structure of carbon aerogel. Among the carbon samples, carbon aerogel activated at 800 °C with a high surface area and a well-developed porous structure exhibited the highest specific capacitance. In addition, carbon aerogel activated at 800 °C retained a considerable specific capacitance at a high current density even after 1000 cycles of charge/discharge. Therefore, it is concluded that carbon aerogel activated with KOH at 800 °C can serve as an efficient electrode material for commercial EDLC with a high power density.

Keywords: Carbon Aerogel, Electric Double Layer Capacitor, Organic Electrolyte, KOH Activation, Activation Temperature

INTRODUCTION

The electric double layer capacitor (EDLC), the so-called supercapacitor, has been applied in electrochemical devices such as memory back up, hybrid electric vehicles, and energy storage systems [1-3]. Because of its unique properties, such as high power density, long life cycle, and fast charge-discharge rate, EDLC is widely used in electric equipment [4,5]. Energy storage mechanism in EDLC is the electrostatic storage of the electrical energy obtained by separation of charge at the interface between the surface of an electrode and an electrolyte [6]. For this reason, the EDLC electrode is required to have a high surface area for ion sorption, well-developed pore structure for the path of ion moving, good conductivity, and wettability for organic or aqueous electrolyte [7].

A number of carbon materials have been intensively investigated as EDLC electrode. In particular, activated carbon has been recommended for commercial EDLC electrode due to its high surface area, chemical inertness, and low cost [8-10]. However, the relatively low conductivity of activated carbon is a serious drawback, so that the specific capacitance of activated carbon is very low at a high charge-discharge current density [11]. To overcome these problems, many carbon materials with high electric conductivity have been attempted for EDLC electrodes, including graphene [12-15], carbon nanotube (CNT) [16-18], and carbon aerogel [19-21]. In this study, carbon aerogel was selected as the electrode material because the physical properties of carbon aerogel can be easily controlled by the preparation conditions such as gelation temperature, pH value, and molar ratio of reactant/catalyst [22].

Carbon aerogel is a mesoporous carbon material derived from gel, in which the liquid of the gel has been replaced with air [23]. Therefore, it has a three-dimensional network structure of carbon particles, resulting in a high electric conductivity, a low density, and other interesting properties [19]. However, a serious drawback of carbon aerogel is that its surface area is much lower than commercial activated carbon. Low surface area of carbon aerogel leads to the limited power and energy densities in EDLC [24].

To increase the surface area of carbon material, various activation methods are generally employed. Activation methods are largely classified as physical activation and chemical activation. Physical activation uses steam or CO_2 gas as activation agents [25-28]. On the contrary, chemical agents such as KOH are generally utilized in chemical activation [29-32]. Chemical activation method was conducted using KOH as activation agent in this study. According to the reported mechanism for chemical activation of carbon material with KOH [29], KOH reacts with carbon material to produce the reduced compounds such as K and K_2CO_3 by the following

†To whom correspondence should be addressed.
E-mail: myungkim@mju.ac.kr, jcjung@mju.ac.kr

equations:

$$6KOH+2C\leftrightarrow 2K+3H_2+2K_2CO_3 \quad (1)$$

$$4KOH+C\leftrightarrow 4K+CO_2+2H_2O \quad (2)$$

$$4KOH+2CO_2\leftrightarrow 2K_2CO_3+2H_2O \quad (3)$$

The K and K_2CO_3 produced in the reduction reaction of KOH could be continuously removed from the reaction site by inert flow during the activation step at high temperature and the subsequent washing process after the activation step. The removal of the reduced compounds facilitates creating new pores, leading to a well-developed pore structure of carbon material. In the chemical activation of carbon material, the activation temperature is known as one of the crucial factors to increase the surface area and to develop the pore structure [31]. However, any systematic investigation to see the effect of activation temperature on the electrochemical properties of carbon aerogel for EDLC electrode in organic electrolyte has not been attempted yet.

In this work, chemical activation of carbon aerogel using KOH was conducted at various temperatures to investigate the effect of activation temperature in chemical activation. For this purpose, carbon aerogel was prepared by a sol-gel method using resorcinol and formaldehyde precursors for polymerization. Activated carbon aerogels were applied to electrode in coin-type EDLC cells using organic electrolyte. Coin-type EDLC cells were assembled using two symmetrical carbon electrodes, and their electrochemical performance was evaluated by cyclic voltammetry, galvanostatic charge/discharge, and electrochemical impedance spectroscopy.

EXPERIMENTAL

1. Material Preparation

Resorcinol ($C_6H_6O_2$, Sigma-Aldrich) and formaldehyde (H_2CO, Sigma-Aldrich) were used as starting materials for preparation of carbon aerogel in ambient conditions. First, two starting materials were polymerized in the aqueous solution to obtain resorcinol-formaldehyde (RF) gel. In the polymerization reaction, sodium carbonate (Na_2CO_3, Sigma-Aldrich) was employed as a base catalyst. Reactants in aqueous were maintained at about 40 wt%. Molar ratio of resorcinol, formaldehyde, and sodium carbonated was fixed at 1 : 2 : 500. The solution was changed into the RF gel in the oven at 80 °C. To remove the water inside the RF gel, solvent exchange was carried out with fresh acetone every 3 hours for 1 day. After the solvent exchanging, the wetted RF gel was dried at room temperature. The dried RF gel was carbonized at 800 °C for 2 h with a nitrogen stream in a tube furnace to yield carbon aerogel. The obtained monolithic carbon aerogel was finally ground for the activation step.

To investigate the effect of activation temperature, chemical activation was conducted at various temperatures in the range of 600-900 °C. Activated carbon aerogel was prepared by the pyrolysis of carbon aerogel with KOH. The mass ratio of carbon aerogel : KOH was fixed at 4 : 1. Carbon aerogel and KOH were physically mixed, and then activated at 600, 700, 800, and 900 °C, respectively, for 2 h under a nitrogen stream. The activated samples were washed with distilled water to remove the remaining KOH and impurities such as K and K_2CO_3. The resulting powder was finally dried at 50 °C overnight. The activated carbon aerogels were denoted as ACA_X (X=600, 700, 800, and 900), where X represents activation temperature.

2. Characterization

Texture properties of the prepared samples were investigated by N_2 adsorption/desorption method at 77K from ASAP 2020 (Micromeritics) instrument. Obtained adsorption/desorption plots were used to calculate the surface areas of the samples by Brunauer-Emmett-Teller (BET) equation and to determine the pore size distributions of the samples using the Barrett-Joyner-Halenda (BJH) method with the desorption branch. SEM analysis (Jeol, JSM-6700F) was conducted to investigate the surface morphology of the samples. Crystal structure of the samples was investigated by XRD measurements (Shimadzu, XRD-7000) using Cu-Kα radiation (λ=1.54056 Å) operated 40 kV and 40 mA.

3. Electrochemical Performance of EDLC Electrode in Organic Electrolyte

Electrochemical performance of the samples was examined using coin-type cell EDLC in organic electrolyte. Electrode was prepared by mixing active material (80 wt%), conductive additive (Super-P, 10 wt%), and binder (Polyvinylidene fluoride, 10 wt%) in 1-methyl-2-pyrrolidone (NMP) to form slurry. Carbon aerogel (CA) and activated carbon aerogels (ACA_X) were used as active materials for EDLC electrode. Electrode sheet was obtained by coating the slurry onto the etched aluminum foil (current collector) using a doctor-blade apparatus. The coated foil was dried in an oven at 70 °C for one day, and then, the dried foil was pressed using a double-roll press at 80 °C.

Coin-type EDLC cells were fabricated using two symmetrical carbon electrodes, separator, and organic electrolyte. The prepared electrode sheet was punched into the small disks with 18 mm diameter, and then it was soaked in organic electrolyte (1 M tetraethylammonium tetrafluoroborate in acetonitrile, $TEABF_4$/AN) for one day in a glove box filled with argon. The sufficiently wetted two electrodes were placed into the coin cells. Separate with a diameter of 19 mm was placed between the same electrodes. Finally, coin-type cell was assembled using a coin cell crimper.

Cyclic voltammetry, galvanostatic charge/discharge, and electrochemical impedance spectroscopy measurement were carried out to investigate the electrochemical properties of the samples. Cyclic voltammetry measurements were conducted at scan rates of 10 mV/s and 100 mV/s with in the voltage range of 0-2.5 V. Charge/discharge measurements were performed at various current loads from 1 to 5 A/g within the same voltage range as cyclic voltammetry measurements. To evaluate the cell resistance, electrochemical impedance spectroscopy (EIS) measurements were also carried out with in the frequency range of 100 kHz to 0.01 Hz at open circuit potential with an AC 5 mV.

RESULTS AND DISCUSSION

1. Physical Properties of Carbon Aerogel (CA) and Activated Carbon Aerogels (ACA_X)

Surface area and pore size distribution of electrode material are well known to be one of the crucial factors to determine its elec-

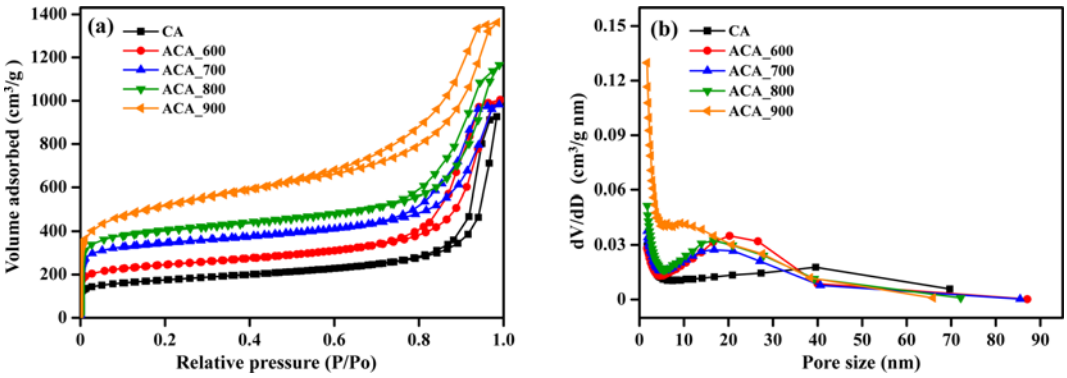

Fig. 1. (a) N_2 adsorption/desorption isotherms and (b) pore size distributions of carbon aerogel (CA) and activated carbon aerogels (ACA_X).

trochemical performance for EDLC [24]. N_2 adsorption/desorption measurements were carried out at 77 K, to investigate the textural properties of carbon aerogel (CA) and activated carbon aerogels (ACA_X). Type IV isotherms with H2 type hysteresis loop were observed in all carbon materials (Fig. 1(a)). What is interesting is that the hysteresis loop of activated carbon aerogels (ACA_X) was shifted to the lower relative pressure with increasing activation temperature (X). This result indicates that average pore size of activated carbon aerogels decreased with increasing activation temperature. To confirm pore size of activated carbon aerogels, pore size distribution plots were obtained from N_2 adsorption/desorption isotherms through the BJH method with desorption branch (Fig. 1(b)). As expected, a higher activation temperature resulted in a lower average pore size of activated carbon aerogel. BET surface area and average pore diameter of activated carbon aerogels are summarized in Table 1. As the activation temperature increased, BET surface area of activated carbon aerogel increased with a smaller average pore size. From the results in N_2 adsorption-desorption analysis, it can be inferred that activation temperature have a strong influence on the textural properties of activated carbon aerogels.

Table 1. Physical properties of carbon aerogel (CA) and activated carbon aerogels (ACA_X)

	Surface area (m^2/g)[a]	Average pore diameter (nm)[b]
CA	628	17.7
ACA_600	895	14.4
ACA_700	1291	12.3
ACA_800	1493	12.4
ACA_900	1860	7.53

[a]Surface area was calculated by the Brunauer-Emmett-Teller (BET) plot

[b]Average pore diameter was determined by the Barret-Joyner-Halenda (BJH) method with the desorption branch

Surface morphology of activated carbon aerogel was observed by SEM analysis. After activation of carbon aerogel with KOH, the morphology of carbon aerogel was obviously changed. As shown

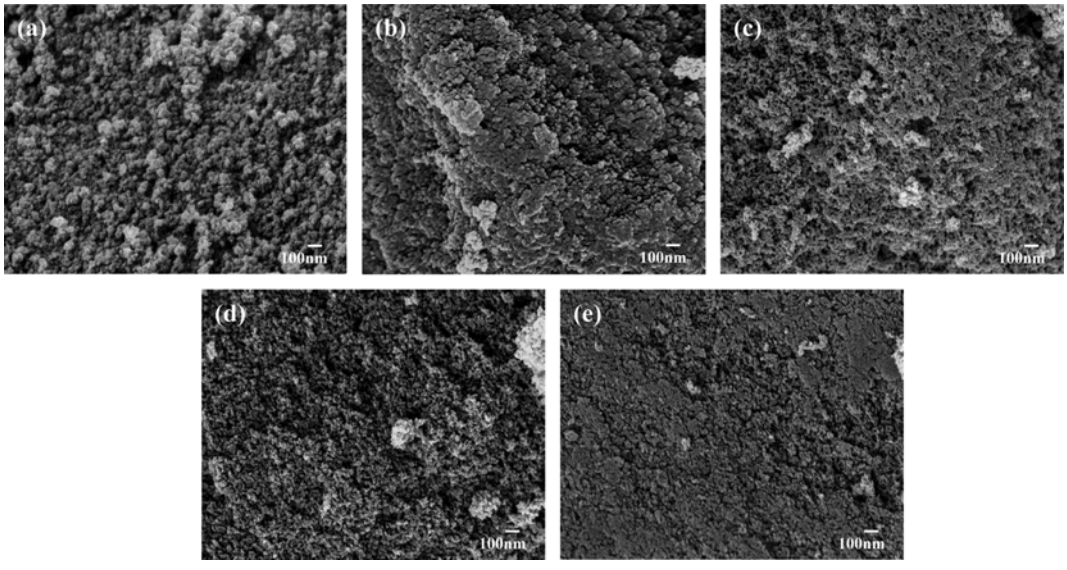

Fig. 2. SEM images of (a) carbon aerogel (CA) and activated carbon aerogels (ACA_X) at the activation temperature (X) of (b) 600 °C, (c) 700 °C, (d) 800 °C, and (e) 900 °C.

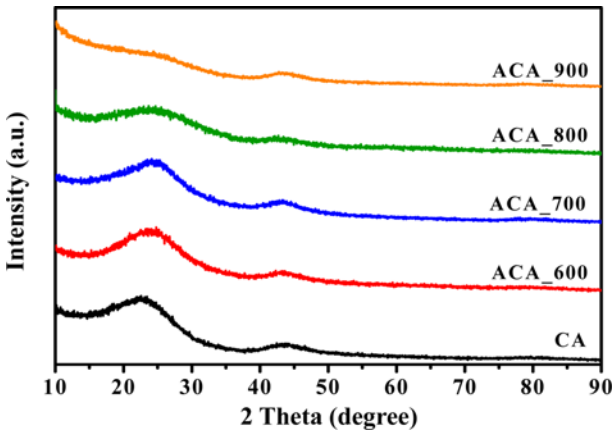

Fig. 3. XRD patterns of carbon aerogel (CA) and activated carbon aerogels (ACA_X).

in Fig. 2(a), carbon aerogel retained an interconnecting network structure of carbon particles with non-uniform textural porosity. With increasing activation temperature up to 800 °C, the three-dimensional 3D network structure of carbon particles and the porous structure of activated carbon aerogels were enlarged and developed, respectively. Note that carbon aerogel activated at 900 °C (ACA_900) exhibited an amorphous carbon structure due to the aggregation of carbon particle during the activation step. The characteristic structure of carbon aerogel is assumed to be collapsed after activation at 900 °C, indicating that excessively high activation temperature can have an adverse effect on the electrochemical properties of carbon aerogel.

XRD patterns of carbon aerogel (CA) and activated carbon aerogels (ACA_X) are shown in Fig. 3. All carbon materials showed two broad characteristic diffraction peaks of graphite carbon at 2θ= 23.5° (002) and 43.8° (001). Therefore, carbon aerogel and activated carbon aerogels could be regarded as a partly graphitized carbon [29]. Interestingly, the peak intensities gradually decreased with increasing activation temperature. This result means that graphitic characteristic of carbon aerogel decreased after activation with KOH, in good agreement with SEM analysis. When considering the high conductivity of graphitic carbon, carbon aerogel activated at excessively high temperature may show a poor electrochemical performance for EDLC electrode at high current density. Consequently, it is believed that optimal activation temperature is required to improve the electrochemical performance of carbon aerogel for EDLC electrode.

2. Electrochemical Performance of Carbon Aerogel (CA) and Activated Carbon Aerogels (ACA_X) by Cyclic Voltammetry and Charge/Discharge Measurements

Cyclic voltammetry and charge/discharge measurements were conducted to evaluate the electrochemical properties and specific capacitances of activated carbon aerogels for EDLC electrode in organic electrolyte. A commercial activated carbon (AC), which is well known as MSP-20 (Kansai Coke & Chemicals Co., Japan), was also investigated as a reference. Specific capacitance of activated carbon aerogels was calculated using the following equation, where I_a and I_c are the anodic current and the cathodic current, respectively. dV/dt is the scan rate and m is the total weight of active carbon material for two electrodes.

$$C = \frac{I_a + |I_c|}{2m \cdot (dV/dt)}$$

All carbon materials showed rectangular, symmetric, and reversible shaped CV curves in the voltage range of 0-2.5 V at a low scan rate (Fig. 4(a)), indicating all samples retained general electrochemical properties of carbon material for EDLC electrode. Among the carbon materials tested, carbon aerogel activated at 800 °C (ACA_800) showed the highest current density within all potential ranges and exhibited the largest integrated area of CV curve (Fig. 4(a)). It is interesting that carbon aerogel activated at 800 °C (ACA_800) retained a larger integrated area of CV curve than commercial activated carbon (AC). When considering the fact that carbon aerogel has a serious drawback for EDLC electrode due to its low surface area compared with commercial activated carbon, a chemical activation with KOH was an efficient method to overcome the shortcoming of carbon aerogel. Although most of CV curves of activated carbon aerogels became narrow and its symmetry decreased with increasing scan rate, ACA_800 maintained the rectangular shaped CV curve even at a high scan rate of 100 mV/s. The excellent capacitance behavior of ACA_800 at a high scan rate implies its low equivalent series resistance (ESR). Specific capacitances of activated carbon

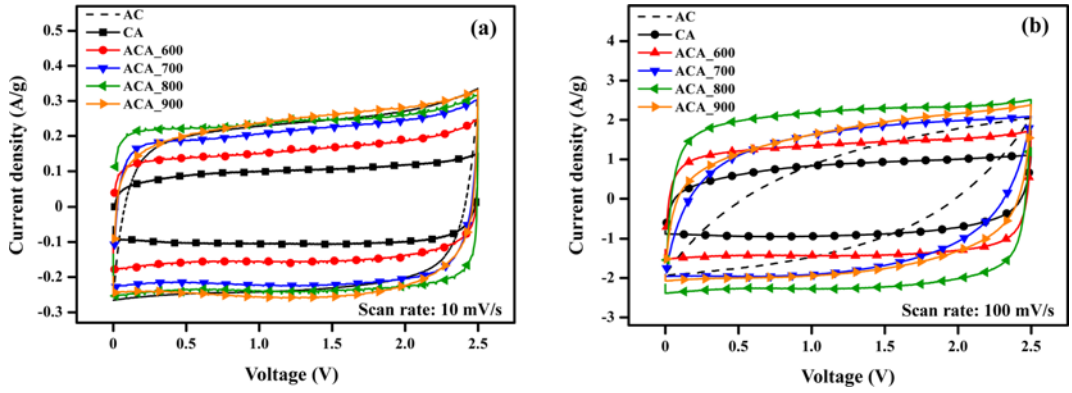

Fig. 4. Cyclic voltammograms of carbon aerogel (CA) and activated carbon aerogels (ACA_X) at a scan rate of (a) 10 mV/s and (b) 100 mV/s (CV curves of commercial activated carbon (AC) were also included for a comparison).

Table 2. Specific capacitances of carbon aerogel (CA) and activated carbon aerogel (ACA_X) determined from CV curve

Scan rate (mV/s)	Specific capacitance (F/g)				
	CA	ACA_600	ACA_700	ACA_800	ACA_900
10	9.9	15.4	20.8	23.6	23.3
100	7.9	13.3	14.6	20.9	16.1

aerogel determined from CV curve are listed in Table 2. As expected, the highest specific capacitance was obtained over ACA_800 electrode.

Galvanostatic charge/discharge measurement was also carried out to confirm the electrochemical properties of all samples. Fig. 5 shows the discharge curve of activated carbon aerogel at a constant current density of 1 A/g, 3 A/g, and 5 A/g. Specific capacitances of the samples were determined by the following equation for discharge curves, and then, results are summarized in Table 3.

$$C = \frac{I \cdot \Delta t}{m \cdot \Delta V}$$

Here, I is the discharge current, Δt is the discharge time, m is the total weight of active carbon material for two electrodes, and ΔV is the operating voltage range during discharging. Activated carbon aerogels showed a longer discharge than carbon aerogel at all current densities, indicative of a larger specific capacitance of activated carbon aerogels for EDLC electrode. This result means that chemical activation with KOH can serve as an efficient way to improve the

Table 3. Specific capacitances (calculated from galvanostatic charge/discharge measurements), R_s (solution resistance), and R_{ct} (charge transfer resistance) of carbon aerogel (CA) and activated carbon aerogels (ACA_X)

	Specific capacitance (F/g)			R_s (ohm)	R_{ct} (ohm)
	1 A/g	3 A/g	5 A/g		
CA	8.7	6.6	5.0	2.4	9.5
ACA_600	14.5	13.8	12.0	3.4	7.2
ACA_700	20.7	16.8	14.0	2.2	4.5
ACA_800	23.3	23.1	21.0	2.6	2.6
ACA_900	21.2	16.5	14.0	2.0	7.3

electrochemical performance of carbon aerogel. It is well known that specific capacitance of carbon material is almost proportional to its surface area [2]. Therefore, it is thought that the enhanced specific capacitance of activated carbon aerogels may be due to the increment of surface area by a chemical activation process.

As shown in Fig. 5 and Table 3, most of activated carbon aerogels experienced a decrement of specific capacitance with increasing current density, which is a general tendency of carbon electrode for EDLC in organic electrolyte. However, carbon aerogel activated at 800 °C (ACA_800) exhibited excellent electrochemical performance with almost no IR drop at a high current density of 5 A/g. The high specific capacitance of ACA_800 at a high current density may be attributed to its high surface area obtained from chemical activation with KOH and well-developed porous structure of

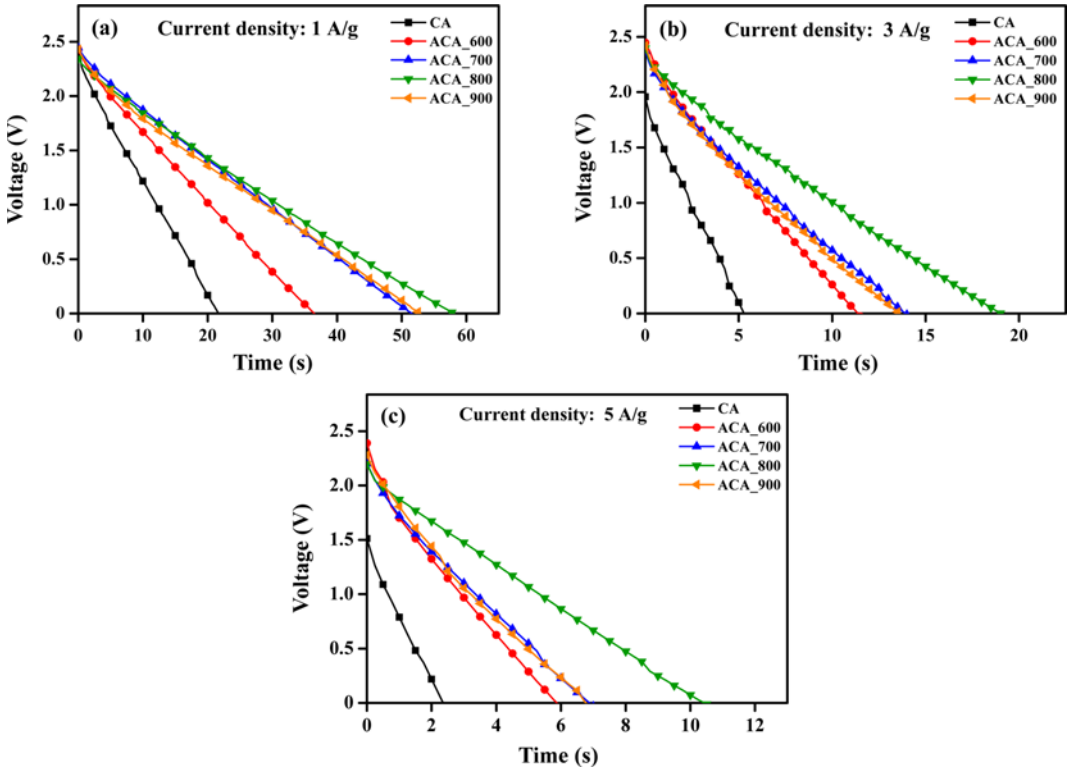

Fig. 5. Charge/discharge profiles of carbon aerogel (CA) and activated carbon aerogels (ACA_X) at a constant current of (a) 1 A/g, (b) 3 A/g, and (c) 5 A/g.

carbon particles. Well-developed porous structure of ACA_800 could be favorable for ion diffusion of organic electrolyte. Although surface area of carbon aerogel activated at 900 °C (ACA_900) is the highest among the carbon samples tested in this work, ACA_900 rather than ACA_800 showed worse electrochemical performance for EDLC electrode in organic electrolyte, especially at a high current density. As we confirmed in SEM and XRD analyses, the network structure of carbon particles disappeared after activation at 900 °C because of the aggregation of carbon particle during the activation step. This resulted in a low electrical conductivity of ACA_900, leading to its low specific capacitance at a high current density.

To confirm the effect of activation temperature on the electrochemical performance of carbon aerogel, we plotted specific capacitance of activated carbon aerogels as a function of activation temperature (Fig. 6). Specific capacitance data were taken from discharge curves measured at a current density of 5 A/g. Specific capacitance of activated carbon aerogel showed a volcano-shaped curve with respect to activation temperature. Among the ACA_X samples, ACA_800 exhibited the highest specific capacitance (21.0 F/g). Once again, we confirmed that activation temperature may be a crucial factor in determining the electrochemical performance of activated carbon aerogel for EDLC electrode.

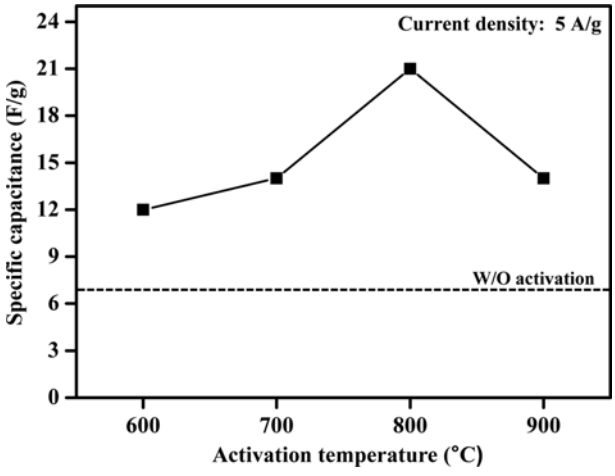

Fig. 6. Specific capacitance of activated carbon aerogels with respect to activation temperature.

3. Electrochemical Characterization by Electrochemical Impedance Spectroscopy

Electrochemical impedance spectroscopy (EIS) analysis was conducted within a frequency range from at 100 kHz to 0.01 Hz. Fig. 7 shows the Nyquist plots of carbon aerogel (CA) and activated carbon aerogels (ACA_X). R_s (solution resistance) and R_{ct} (charge transfer resistance) determined from Nyquist plot are summarized in Table 3. The Nyquist plot consists of a semi-circle loop at a high frequency and a straight line at a low frequency, indicative of the charge transfer resistance and the Warburg response, respectively. The first intersection on real axis of the plot indicates the bulk solution resistance (R_s). It is known that R_s is different depending on the electrolyte conductivity and the identity of the separator [33]. R_{ct}, which can be determined from the radius of a semi-circular loop, comes from two factors: the electronic and the ionic resistances. The electronic resistance includes the intrinsic resistance of electrode material and the contact resistance between the active layer and the current collector. The ionic resistance is related to the electrolyte ionic conductivity inside the pores of electrode [33].

Among the activated carbon aerogels tested in this work, the radius of the semi-circular loop of ACA_800 was the smallest (Fig. 7), indicating the lowest charge transfer resistance of ACA_800. As expected, ACA_900 has a larger radius of semi-circular loop than ACA_800 because of the collapse of three-dimensional network structure and porous structure during the activation step at 900 °C. From the EIS analysis, it is again confirmed that the enhanced electrochemical performance of ACA_800 at a high current density was attributed to its low electrical resistance resulting from a well-developed porous structure.

4. Cycle Stability Test

To examine the cycle stability of activated carbon aerogel electrode, a charge/discharge cycle test was conducted with coin-cell type EDLC cell fabricated using ACA_800 as an electrode material. Current density was maintained at 5 A/g and specific capaci-

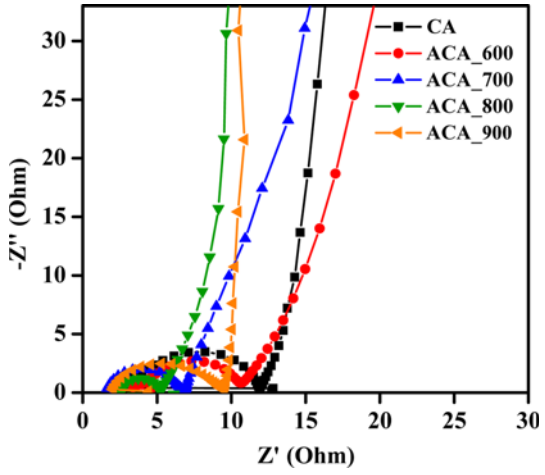

Fig. 7. Nyquist plots of carbon aerogel (CA) and activated carbon aerogels (ACA_X).

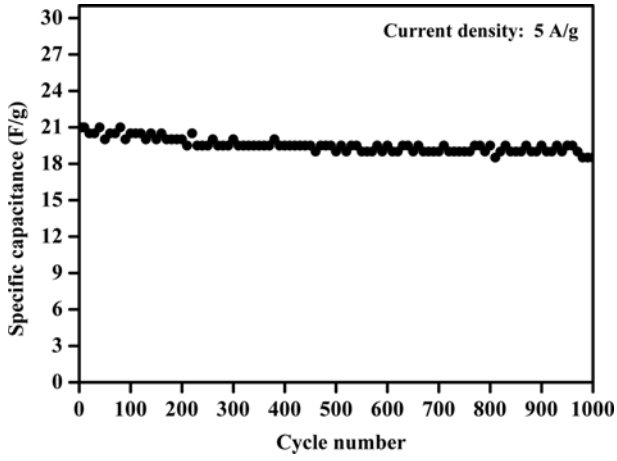

Fig. 8. Cycle stability of ACA_800 electrode for EDLC in organic electrolyte.

tance was determined from the discharge curve. As shown in Fig. 8, ACA_800 showed good stability during the cycle test. Even after 1000 cycles of charge/discharge, ACA_800 retained a considerable specific capacitance compared to the initial cycles. Therefore, it can be concluded that carbon aerogel activated at 800 °C can serve as an efficient electrode material for commercial EDLC with a high power density.

CONCLUSIONS

Carbon aerogel was prepared by a poly-condensation of resorcinol and formaldehyde, and then, it was chemically activated with KOH at various activation temperatures to improve its electrochemical properties. Surface area of activated carbon aerogels increased with increasing activation temperature. However, the three-dimensional network structure and the porous structure of carbon aerogel were enlarged and developed, respectively, with increasing activation temperature up to 800 °C. Carbon aerogel activated at 900 °C (ACA_900) exhibited an amorphous carbon structure due to the aggregation of carbon particle during the chemical activation with KOH, leading to a loss of unique structure of carbon aerogel.

Coin-type EDLC cells were fabricated using the activated carbon aerogels with the aim of evaluating their electrochemical performance for EDLC electrode in organic electrolyte. Activated carbon aerogels showed a higher specific capacitances than carbon aerogel, indicating that chemical activation with KOH served as an efficient method to improve the electrochemical performance of carbon aerogel. However, ACA_900 rather than ACA_800 showed a lower specific capacitance at a high current density due to the high charge transfer resistance. This means that activation temperature played a key role in determining the electrochemical performance of activated carbon aerogel for EDLC electrode. Among the activated carbon aerogels, ACA_800 exhibited the highest specific capacitance with good cycle stability. The enhanced electrochemical performance of ACA_800 at a high current density was due to its high surface area and well-developed porous structure obtained from chemical activation with KOH.

ACKNOWLEDGEMENTS

This work was supported by the World-Class 300 Project funded by the Small and Medium Business Administration of Korea (SMBA).

REFERENCES

1. P. Sharma and T. S. Bhatti, *Energy Convers. Manage.*, **51**, 2901 (2010).
2. E. Frackowiak, Q. Abbas and F. Béguin, *J. Energy Chem.*, **22**, 226 (2013).
3. S. L. Candelariaa, Y. Shao, W. Zhouc, X. Li, J. Xiao, J.-G. Zhang, Y. Wang, J. Liu, J. Li and G. Cao, *Nano Energy*, **1**, 195 (2012).
4. M.-G. Jeong, K. Zhuo, S. Cherevko and C.-H. Chung, *Korean J. Chem. Eng.*, **29**, 1802 (2012).
5. A. Thambidurai, J. K. Lourdusamy, J. V. John and S. Ganesan, *Korean J. Chem. Eng.*, **31**, 268 (2014).
6. E. Frackowiak and F. Béguin, *Carbon*, **39**, 937 (2001).
7. L. Wei and G. Yushin, *Nano Energy*, **1**, 552 (2012).
8. E. Jeong, M.-J. Jung, S. H. Cho, S. I. Lee and Y.-S. Lee, *Colloids Surf., A*, **377**, 243 (2011).
9. A. Elmouwahidi, Z. Zapata-Benabithe, F. Carrasco-Marin and C. Moreno-Castilla, *Bioresour. Technol.*, **111**, 185 (2012).
10. Y. Zhang, H. Feng, X. Wu, L. Wang, A. Zhang, T. Xia, H. Dong, X. Li and L. Zhang, *Int. J. Hydrogen Energy*, **34**, 4889 (2009).
11. Y. Guo, Z.-q. Shi, M.-m. Chen and C.-y. Wang, *J. Power Sources*, **252**, 235 (2014).
12. Y. Huang, J. Liang and Y. Chen, *Small*, **8**, 1805 (2012).
13. S. R. C. Vivekchand, C. S. Rout, K. S. Subrahmanyam, A. Govindaraj and C. N. R. Rao, *J. Chem. Sci.*, **120**, 9 (2008).
14. S. D. Perera, A. D. Liyanage, N. Nijem, J. P. Ferraris, Y. J. Chabal and K. J. Balkus Jr., *J. Power Sources*, **230**, 130 (2013).
15. Z.-S. Wu, G. Zhou, L.-C. Yin, W. Ren, F. Li and H.-M. Cheng, *Nano Energy*, **1**, 107 (2012).
16. S.-H. Yoon, S. Lim, Y. Song, Y. Ota, W. Qiao, A. Tanaka and I. Mochida, *Carbon*, **42**, 1723 (2004).
17. J. Zhong, Z. Yang, R. Mukherjee, A. V. Thomas, K. Zhu, P. Sun, J. Lian, H. Zhu and N. Koratkar, *Nano Energy*, **2**, 1025 (2013).
18. Z. Niu, P. Luan, Q. Shao, H. Dong, J. Li, J. Chen, D. Zhao, L. Cai, W. Zhou, X. Chen and S. Xie, *Energy Environ. Sci.*, **5**, 8726 (2012).
19. R. W. Pekala, J. C. Farmer, C. T. Alviso, T. D. Tran, S. T. Mayer, J. M. Miller and B. Dunn, *J. Non-Cryst. Solids*, **225**, 74 (1998).
20. X. Wu and W. Jia, *Chem. Eng. J.*, **245**, 210 (2014).
21. C. Robertson, *Micropor. Mesopor. Mater.*, **179**, 151 (2013).
22. S.-W. Hwang and S.-H. Hyun, *J. Non-Cryst. Solids*, **347**, 238 (2004).
23. X. Wang, X. Wang, L. Liu, L. Bai, H. An, L. Zheng and L. Yi, *J. Non-Cryst. Solids*, **357**, 793 (2011).
24. Y. J. Lee, G.-P. Kim, Y. Bang, J. Yi, J. G. Seo and I. K. Song, *Mater. Res. Bull.*, **50**, 240 (2014).
25. K. Xia, Q. Gao, J. Jiang and J. Hu, *Carbon*, **46**, 1718 (2008).
26. J. M. V. Nabaisa, P. Nunes, P. J. M. Carrott, M. M. L. R. Carrott, A. M. García and M. A. Díaz-Díez, *Fuel Process. Technol.*, **89**, 262 (2008).
27. S.-Y. Lee and S.-J. Park, *J. Solid State Chem.*, **207**, 158 (2013).
28. Ö. Şahin and C. Saka, *Bioresour. Technol.*, **136**, 163 (2013).
29. S.-Y. Lee and S.-J. Park, *J. Colloid Interface Sci.*, **389**, 230 (2013).
30. L. K. C. de Souza, N. P. Wickramaratne, A. S. Ello, M. J. F. Costa, C. E. F. da Costa and M. Jaroniec, *Carbon*, **65**, 334 (2013).
31. X.-Y. Zhao, S.-S. Huang, J.-P. Cao, S.-C. Xi, X.-Y. Wei, J. Kamamoto and T. Takarada, *J. Anal. Appl. Pyrol.*, **105**, 116 (2014).
32. B. Xu, F. Wu, Y. Sub, G. Cao, S. Chen, Z. Zhou and Y. Yang, *Electrochim. Acta*, **53**, 7730 (2008).
33. C. Lei, F. Markoulidis, Z. Ashitaka and C. Lekakou, *Electrochim. Acta*, **92**, 183 (2013).